

Nonlinear resonant tunneling of Bose-Einstein condensates in tilted optical lattices

K. Rapedius,^{1,2} C. Elsen,¹ D. Witthaut,³ S. Wimberger,⁴ and H. J. Korsch¹

¹*Department of Physics, Technische Universität Kaiserslautern, D-67653 Kaiserslautern, Germany*

²*Center for Nonlinear Phenomena and Complex Systems, Université Libre de Bruxelles, Code Postal 231, Campus Plaine, B-1050 Brussels, Belgium*

³*Network Dynamics Group, Max-Planck-Institute for Dynamics and Self-Organization, D-37073 Göttingen, Germany*

⁴*Institut für theoretische Physik and Center for Quantum Dynamics, Universität Heidelberg, D-69120 Heidelberg, Germany*

(Received 18 May 2010; published 3 December 2010)

We study the tunneling decay of a Bose-Einstein condensate from tilted optical lattices within the mean-field approximation. We introduce a method to calculate ground and excited resonance eigenstates of the Gross-Pitaevskii equation, based on a grid relaxation procedure with complex absorbing potentials. This algorithm works efficiently in a wide range of parameters where established methods fail. It allows us to study the effects of the nonlinearity in detail in the regime of resonant tunneling, where the decay rate is enhanced by resonant coupling to excited unstable states.

DOI: 10.1103/PhysRevA.82.063601

PACS number(s): 03.75.Lm, 03.65.Ge, 03.65.Nk

I. INTRODUCTION

The dynamics of a quantum particle in a periodic potential subject to an external force is one of the central problems in solid-state physics. In the field free case all eigenstates are delocalized over the lattices, leading to transport [1,2]. The application of a constant force leads to a localization of the eigenstates such that transport is suppressed contrary to our intuition [3–6]. Instead, the quantum particle performs the celebrated Bloch oscillations and eventually decays by repeated Zener tunneling to higher Bloch bands [7–18]. The most detailed studies of Bloch oscillations and decay have been carried out with ultracold atoms trapped in optical lattices. These systems are particularly appealing, because the dynamics of the atoms can be recorded in situ and all parameters can be tuned precisely over a wide range. The external force can be induced by gravity [7], magnetic gradient fields [8], or accelerating the lattice [9–14]. Decay in strong fields manifests itself in the pulsed output of coherent matter waves. The dynamics is even more interesting when the atoms undergo Bose-Einstein condensation and interactions have to be taken into account. For low temperature and high densities, the dynamics of the atoms can be described by the celebrated Gross-Pitaevskii equation (GPE) with astonishing accuracy [19]. In this treatment, interactions are incorporated by a nonlinear mean-field potential, which is proportional to the condensate density. The nonlinearity of the equation alters the dynamics and in particular the decay substantially. Interactions can lead to a damping of Bloch oscillations [20], asymmetric Landau-Zener tunneling [10,21,22], or a bistability of resonance curves [23–25].

Here we study the resonance eigenstates of the GPE

$$\left(\frac{-\hbar^2}{2m} \frac{d^2}{dx^2} + V(x) + Fx + g|\psi(x)|^2 \right) \psi(x) = (\mu - i\Gamma/2)\psi(x) \quad (1)$$

with a periodic potential $V(x+d) = V(x)$ and a static force $F > 0$, which is known as a Wannier-Stark (WS) potential. The imaginary part Γ of the eigenenergy gives the decay rate of the condensate. A comprehensive review of the localized eigenstates, the WS resonances, can be found in Ref. [17]. In

the following we assume a cosine potential $V(x) = V_0 \cos(x)$ except for Sec. IV, where a bichromatic lattice is considered. Throughout this article we use scaled units defined by $\tilde{x} = 2\pi x/d$ such that the period of the potential is 2π and $\hbar = m = 1$. The energies, μ and V_0 , are then given in units of $8E_R$, where $E_R = (\hbar^2 \pi^2)/(2md^2)$ is the recoil energy. If not stated otherwise we fix the strength of the lattice as $V_0 = 1$ in scaled units.

In this article we introduce an algorithm for the computation of nonlinear resonance states based on a grid relaxation method with a complex absorbing potential (CAP). This algorithm converges in a wide parameter range and is applicable even to situations of many degenerate energy levels, such as the WS system at resonance condition (see below). It is thus capable to describe genuine nonlinear phenomena such as bistability, which pose a major difficulty to other methods as for instance nonlinear complex scaling (CS) [26–31]. In addition, it is more efficient and easier to implement and, unlike previous methods, is not restricted to ground-state calculations but can also compute excited states. Note that our approach differs from the CAP method used in Refs. [27,32] because the latter does not use a grid relaxation but relies on a basis set expansion. Although such expansions work well for simple single-well potentials, they cannot easily handle complicated problems like the Wannier-Stark system studied in the present article, which requires the use of as much as 500 basis states even in the linear (noninteracting) case [33]. Our method is applied to study the decay of a Bose-Einstein condensate in the strongly nonlinear regime. Nonlinear effects are crucial in the regime of resonantly enhanced tunneling (RET). In this case a metastable WS resonance becomes energetically degenerate with an excited, less stable state, which can increase the decay rate by orders of magnitude. This phenomenon is most pronounced in deep optical lattices and has been studied systematically for the linear case in Refs. [16,17]. The nonlinearity shifts the resonance and eventually bends the resonance peak leading to a bistable behavior.

II. COMPUTATIONAL METHOD

Linear WS resonances can be efficiently calculated with the truncated shift operator technique introduced in Ref. [33].

In the nonlinear case, the method of CS has been applied [26,28–30]. Though satisfactory from a conceptual point of view, this method has several drawbacks. The implementation is complicated as it requires switching between different basis sets as well as different time propagation methods. Furthermore, the calculation of excited states is highly nontrivial, as the method relies on an imaginary time propagation, and the convergence is quite slow, especially for weak fields and close to energetic degeneracies as present in the RET condition [28,29].

As an alternative, we propose a method based on complex absorbing potentials (CAP) performed on a finite grid $[x_-, x_+]$ in real space. We assume that the resonance wave function is mainly localized in the interval $[x_\ell, x_r]$ with $x_- < x_\ell < x_r < x_+$ and fix the normalization as $\int_{x_\ell}^{x_r} |\psi(x)|^2 dx = 1$. For $x \rightarrow -\infty$, we apply a CAP of the type

$$V_{\text{CAP}} \propto \begin{cases} -i(x/x_-)^{10} & x < 0 \\ 0 & x > 0 \end{cases}, \quad (2)$$

which only modifies the wave function in the vicinity of the grid boundary x_- making it square integrable. We choose x_- to be quite large (ca. 40 lattice periods) in order to include enough of the asymptotic behavior of the resonance. The exact size of the area of integration and the strength η of the CAP must be chosen such that the results are stable with respect to a small variation of these parameters (compare the cusp condition in Ref. [34]). On our finite grid $[x_-, x_+]$ the boundary conditions for the wave function read

$$\psi(x_-) = 0, \quad \psi(x_+) = 0, \quad \psi'(x_+) = C, \quad (3)$$

where the last condition is used to control the normalization. The algorithm starts from the linear case $g = 0$, for which all WS resonances can be computed efficiently [33]. Nonlinear WS resonances in different bands are calculated by choosing a different initial guess. The nonlinearity is then increased gradually, using the previous result as initial guess for a standard boundary value problem (BVP) solver, e.g., the MATLAB function `bvp4c`. Applying the BVP solver changes the normalization of ψ , such that the parameter C has to be adjusted according to

$$C \rightarrow C / \left(\int_{x_\ell}^{x_r} |\psi(x)|^2 dx \right)^{1/2}. \quad (4)$$

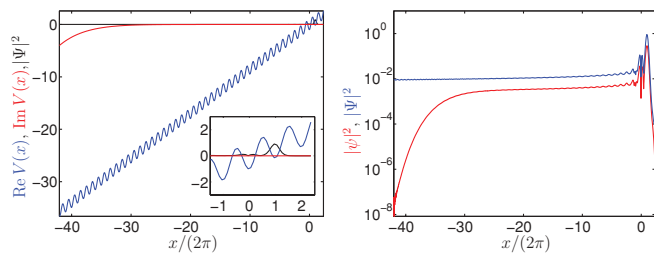


FIG. 1. (Color online) Test of the algorithm for vanishing nonlinearity $g = 0$. (Left panel) Initial solution $|\Psi|^2$ and complex potential $V(x) = \cos(x) + Fx - i\eta(x/x_-)^{10}$ with $F = 0.135$. The inset shows a magnification in the vicinity of the main peak of the initial solution. (Right panel) Comparison between the initial solution $|\Psi|^2$ (blue) and the solution $|\psi|^2$ (red) obtained using a complex absorbing potential.

TABLE I. Decay rates Γ for the most stable resonance of the potential $V(x) = \cos(x)$, taken from Ref. [28] (CS method) and computed using the CAP grid relaxation method. Particularly for small decay rates the new CAP method proves more efficient than the CS technique.

g	F	Γ_{CS}	Γ_{CAP}
0	0.5	1.941×10^{-2}	1.941×10^{-2}
0.1	0.5	2.180×10^{-2}	2.180×10^{-2}
0	0.25	7.2×10^{-4}	7.104×10^{-4}
0.1	0.25	8.4×10^{-4}	8.346×10^{-4}
0.2	0.25	9.7×10^{-4}	9.688×10^{-4}
0.25	0.25	1.04×10^{-3}	1.041×10^{-3}
0.5	0.25	1.48×10^{-3}	1.476×10^{-3}
0.2	0.15	2.9×10^{-5}	2.832×10^{-5}
0.2	0.13125	5.7×10^{-5}	5.600×10^{-5}

This is repeated until the normalization converges to unity. The nonlinearity is then increased by one step.

The basic features of this algorithm and the effects of the CAPs are illustrated in Fig. 1 for a tilted cosine potential with $V_0 = 1$, $F = 0.135$, and $g = 0$. The left-hand side shows the squared magnitude $|\Psi|^2$ of the initial wave function as well as the real and imaginary part of the potential. The right panel of Fig. 1 compares the squared magnitudes of the initial wave function Ψ and the normalized wave function ψ calculated by the BVP solver for the most stable resonance. We observe a difference in the asymptotic behavior for $x \rightarrow -\infty$ which is caused by the CAP. The shift between the two functions is an artifact of a slight difference in normalization caused by the relatively coarse mesh used for the initial solution.

To demonstrate the validity of the CAP algorithm we compare the calculated decay rates for a cosine potential for several parameters to complex scaling results, which themselves were tested against a direct time propagation in Ref. [28]. The values summarized in Table I show an excellent agreement over the entire parameter range. Residual numerical errors are very small; they can mainly be attributed to the limited computation time for the CS method and reflections of the matter wave at the CAP. For a further discussion of CAPs in the simulation of few boson systems, see Ref. [35] and references therein.

III. RESONANTLY ENHANCED TUNNELING

We use the CAP method to investigate how a nonlinear interaction affects the decay of a BEC in a tilted optical lattice. In the weakly interacting regime, the scaling of the decay rate with the field strength is given by the celebrated Landau-Zener formula

$$\Gamma(F) \approx F \exp(\pi \Delta E^2 / F), \quad (5)$$

where ΔE is the energy gap between the Bloch bands of the periodic potential [2,15] and the field strength F determines the oscillation frequency in the bands [15,17]. Major differences

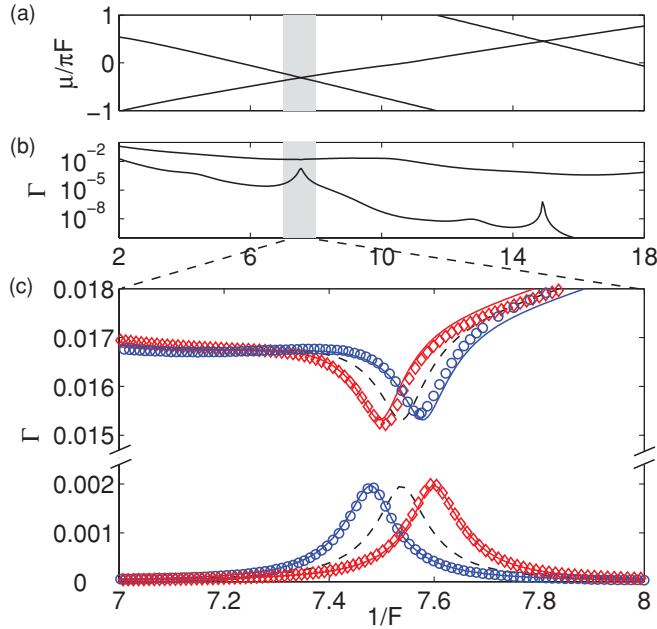


FIG. 2. (Color online) Resonantly enhanced tunneling (RET) of (non-) linear WS resonances. (a) Energies and (b) decay rates of the two most stable WS resonances in a cosine potential as a function of the inverse field strength $1/F$. (c) Shift of the RET peaks due to the nonlinear interaction of a BEC for $g = +0.02$ (\circ), $g = -0.02$ (\diamond), and $g = 0$ (---). Numerical results (symbols) are compared to a perturbative calculation (solid lines) according to Eqs. (6) and (8).

arise in the regime of RET. In this case an eigenstate localized mainly in one of the wells of the potential becomes energetically degenerate with an excited state in another well, which can increase the decay rate by orders of magnitude [17]. In the following, we focus on the experimentally studied regime [11,12], where a modest nonlinearity strongly affects the decay of the condensate [11,12,18].

RET is illustrated in Figs. 2(a) and 2(b) for the linear case $g = 0$, showing the decay rate Γ and the chemical potential μ of the two most stable resonances as a function of F . RET is observed at $1/F \approx 7.5$, where the two energy levels $\mu(F)$ cross. The resonant coupling to the excited states leads to a pronounced RET peak of the decay rate for the most stable resonance. Coincidentally, a pronounced dip is observed for the first excited resonance, which is stabilized by the coupling to the most stable resonance [17]. The influence of a small nonlinearity is illustrated in Fig. 2(c). Three main effects are observed: a shift of the resonance peaks, an increase (decrease) of the peak decay rate in the ground state for $g > 0$ ($g < 0$), and a deformation of the peak shape.

The shift and the deformation can be qualitatively understood by a perturbative approach [28]. To first order, this predicts a shift of the real part of the eigenenergy,

$$\Delta\mu(g) \approx g \int_{x_\ell}^{x_r} |\psi_g|^2 |\psi_{g=0}|^2 dx \approx g \int_{x_\ell}^{x_r} |\psi_{g=0}|^4 dx, \quad (6)$$

which corresponds to a shift of the field strength according to

$$\Delta F(g) \approx \pm \Delta\mu(g)/(2\pi). \quad (7)$$

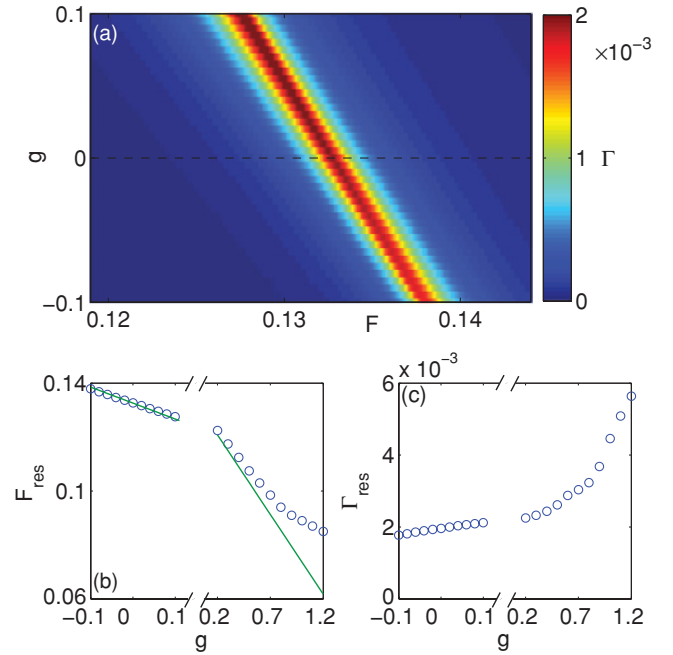


FIG. 3. (Color online) (a) Colormap plot of the decay rates of the most stable WS resonances in a cosine-potential vs. the field strength F and the interaction strength g in the vicinity of the first order RET peak. (b) Position and (c) height of the RET peak vs. the interaction strength g .

Here, the minus sign holds for the ground and the plus sign for the excited band. The nonlinear decay rate is then approximately given by

$$\Gamma_g(F) = \Gamma_0[F + \Delta F(g)]. \quad (8)$$

The shift is further investigated in Fig. 3(b), where the decay rate as well as the peak position is plotted vs. the interaction strength over a wide parameter range. The perturbative calculation (6) predicts that the peak position F_{res} is shifted with a slope $dF_{\text{res}}/dg = 0.059$ for small values of g , which is plotted as a green line in Fig. 3(b). This deviates from the numerically exact results already for small values of g , for which a linear fit yields a smaller slope of $dF_{\text{res}}/dg = 0.051$. In agreement with Ref. [28] we thus find that first-order perturbation theory is insufficient in describing the shift of the RET peaks quantitatively. Noticeably, the RET peak and the dip of the decay rate for the first excited resonance always shift into opposite directions, as shown in Fig. 2(c).

The change in the maximum decay rate is not predicted by perturbation theory but easily explained phenomenologically. It is a direct consequence of the interaction as repulsion between the particles in general leads to a destabilization, whereas attraction leads to a stabilization of both resonances and bound states (see Ref. [10] and references therein). This is further illustrated in Fig. 3(c), where the peak decay rate of the most stable resonance is plotted as a function of g over a wide parameter range. Similar effects have been investigated for several other model potentials [24,26,29,31].

The dependence of the linear and nonlinear RET peaks is further analyzed in Fig. 4. The upper panel shows the decay rate $\Gamma(F)$ for different values of the potential strength V_0 for $g = 0$.

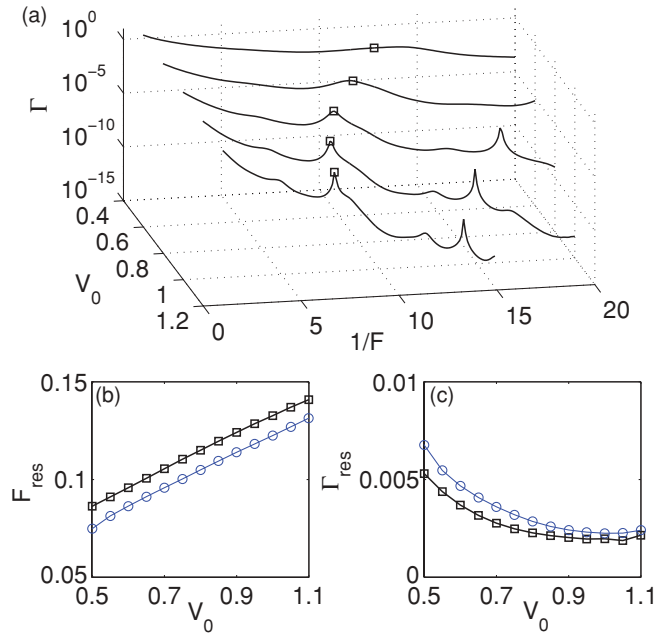


FIG. 4. (Color online) (a) Emergence of the RET peaks: Decay rate Γ as a function of the field strength F for different values of the lattice strength V_0 and $g = 0$. The primal RET peaks analyzed in the following are marked with a square (\square). [(b) and (c)] Scaling of the peak position F_{res} and the peak decay rate Γ_{res} with the strength of the optical lattice V_0 for $g = 0$ (\square) and $g = 0.2$ (\circ).

For shallow lattices, $\Gamma(F)$ decreases monotonically with $1/F$ as predicted by the celebrated Landau-Zener formula (5). As the lattice becomes deeper, Landau-Zener theory predicts that Γ vanishes exponentially with the band width ΔE . However, this is only true as long as tunneling to excited states in neighboring potential wells is not resonantly enhanced. On resonance, the decay rate Γ decreases much slower with V_0 as shown in Fig. 4(c) such that sharp RET peaks emerge. This remains true also for weak nonlinearities as shown for $g = 0.2$ in the figure. One observes a similar slow decrease of Γ_{res} with V_0 , however, the actual values of the decay rate are larger for $g > 0$. The position of the RET peaks F_{res} is plotted as a function of V_0 in Fig. 4(b). Tunneling becomes resonant when ndF matches the energy difference between the most stable and an excited, less stable resonance, where nd is an integer multiple of the lattice period. For a deep lattice this energy difference, and thus also the peak position F_{res} , is given by $\sqrt{V_0}$ [11]. This estimate agrees very well with the numerical results for the linear case $g = 0$ as shown in the figure. In the nonlinear case the RET peaks are shifted to smaller values of the field strength F according to Eq. (7); however, the general progression with the potential strength V_0 remains the same.

Another important feature observed in Fig. 2(c) is that the RET peaks become asymmetric for $g \neq 0$. For a repulsive (attractive) nonlinearity, the peak bends to higher (lower) values of F . If the nonlinearity is increased above a critical value g_{cr} , the peaks bend over and a bistable behavior emerges. The detailed shape of a bistable RET peak is plotted in Fig. 5, which also indicates how WS states are calculated numerically in the bistable regime: We have started with a small value of F which was then gradually increased, using

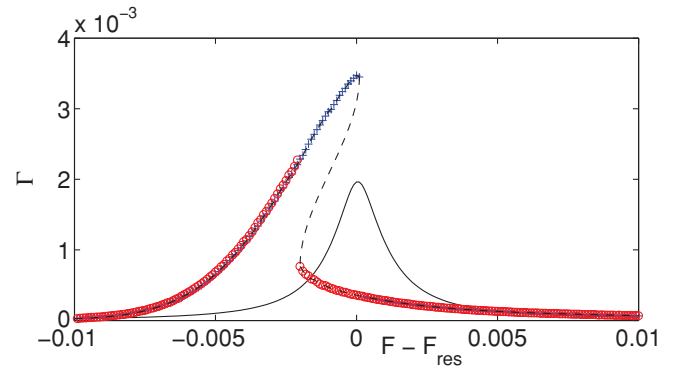


FIG. 5. (Color online) Bistability of the RET peak for strong repulsive interactions ($g = 0.8$). The decay rate was calculated for a forward sweep (blue asterisk) and a backward sweep (red circles). A spline interpolation (dashed line) is included to guide the eye. The solid line shows the linear ($g = 0$) peak shape for comparison.

every result as initial guess for the next calculation (cf. also Refs. [28,29]). After reaching a final, large value of the field strength, the procedure was reversed and F was decreased back to the initial value. Within the regime of bistability forward and backward sweep yield the upper and lower branches of the peak, respectively. The intermediate branch is generally difficult to compute as it is dynamically unstable.

The bending of the RET peak and the emergence of a bistability can be understood qualitatively by the perturbative approach introduced above. A common WS state in a deep optical lattice is strongly localized in a single potential well so its chemical potential is strongly changed according to Eq. (8). In comparison, the state corresponding to the maximum of the RET peak is delocalized because of the energetical degeneracy with an excited state in another well. Therefore its chemical potential is affected rather weakly and according to Eq. (7) also the change of the peak position ΔF is small (cf. also Refs. [11,12]). With increasing nonlinearity, the edges of a RET peak shift to smaller values of the field strength, while the maximum falls behind. The whole peak bends to the right and finally becomes bistable.

The onset of bistability is analyzed quantitatively in Fig. 6. The upper panel shows the two branches of the decay curves for $V_0 = 1$ and different values of g . The RET peaks are shifted to smaller values of F when g is increased and the peaks are bistable for $g = 0.5$ and higher. The lower panel shows the critical nonlinearity g_{cr} as a function of the lattice strength V_0 . The sharp decrease of g_{cr} for $V_0 \gtrsim 1$ can be understood from the properties of the two most stable Wannier-Stark resonance states. Generally, the critical nonlinearity for a bifurcation of a nonlinear stationary state is smallest, when the state is coupled to a second state which is energetically close—a result which has been established quantitatively for nonlinear two-state systems (see Refs. [21,30] and references therein). For $V_0 \gtrsim 1$, the optical lattice becomes deep enough such that the first excited WS resonance state becomes strongly localized and that its decay rate decreases significantly. Correspondingly, the most stable resonance is destabilized as the coupling between the two states is increased – its decay increases for $V_0 \gtrsim 1$ as shown in Fig. 4(c). Furthermore, the coupling to the first

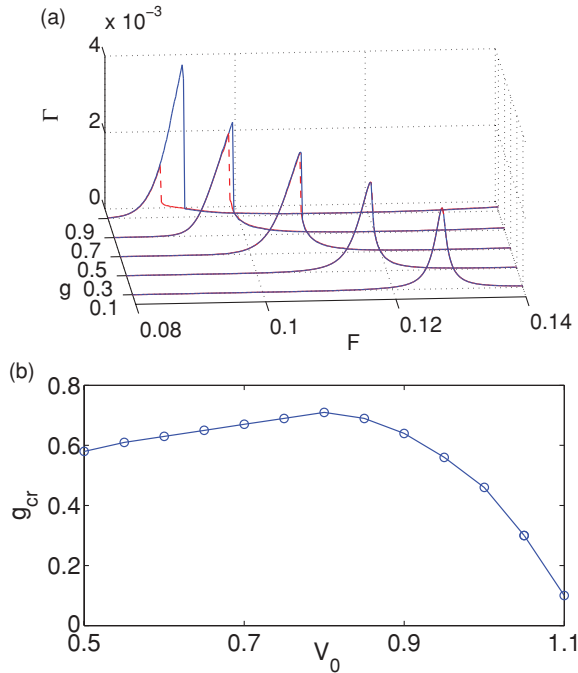


FIG. 6. (Color online) Emergence of bistability of the RET peaks in an optical lattice. (a) Decay rate Γ as a function of the field strength F for different values of the nonlinearity g . The decay rate was calculated for a forward sweep (blue solid lines) and a backward sweep (red dashed lines). (b) Critical nonlinearity g_{cr} for the onset of bistability as a function of the lattice strength V_0 . The solid line is drawn to guide the eye.

excited resonance, which is now energetically close, facilitates a bifurcation and thus the onset of bistability.

The emergence of bistability has also been analyzed for the transmission coefficient in the context of nonlinear RET through one-dimensional potential barriers [23–25]. However, in this case states corresponding to the transmission maximum are localized strongest. Thus the resonance peaks bend into the same direction as they are shifted, which is in contrast to the behavior of the WS RET peaks shown in Fig. 5.

IV. BEYOND THE RET REGIME

A new regime of RET can be explored in bichromatic optical lattices,

$$V(x) = V_0\{\cos(x) + \delta \cos(x/2 + \phi)\}. \quad (9)$$

These potentials can be realized experimentally by superimposing two incoherent optical lattices [36,37] or by combining optical potentials based on virtual two-photon and four-photon processes [38]. The introduction of an additional potential with a doubled periodicity leads to the splitting of the ground Bloch band into two minibands for $F = 0$. This distinguished feature has been used to study Landau-Zener tunneling between different minibands [39] and the interplay of tunneling and Bloch oscillations [40].

The decay rates of the WS resonance states in a bichromatic optical lattice are plotted in Fig. 7(a) as a function of the field strength F for $V_0 = 1$ and $\phi = \pi/2$. The splitting of the Bloch bands into minibands translates into a splitting

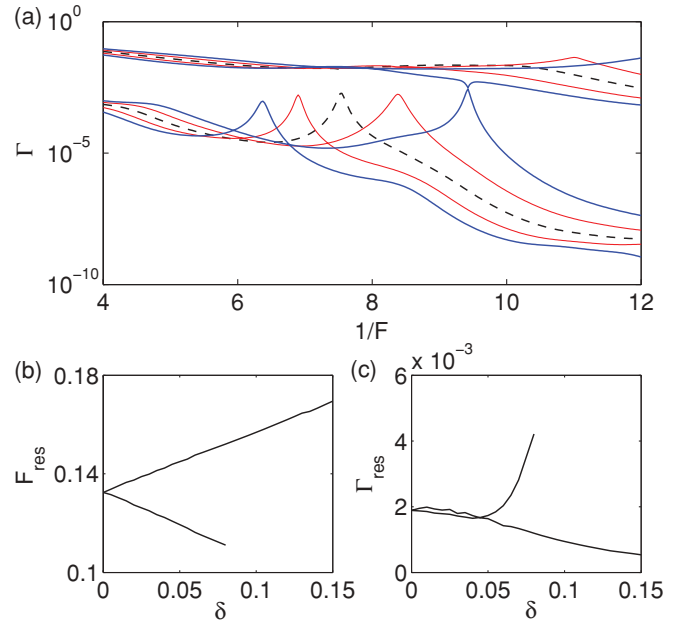


FIG. 7. (Color online) (a) The decay rate Γ of the four most stable WS resonance states in a tilted bichromatic potential (9) for $V_0 = 1$, $\phi = \pi/2$, and $\delta = 0$ (black dashed line), $\delta = 0.05$ (thin red line), and $\delta = 0.1$ (solid blue line). [(b) and (c)] Position F_{res} and height Γ_{res} of the RET peaks of the two most stable resonance states as a function of δ .

of the WS resonance states and their decay curves $\Gamma(F)$, which is most pronounced in the vicinity of the RET peaks. The position of the RET peaks changes linearly with the strength δ of the additional lattice as shown in Fig. 7(b). For $\phi = \pi/2$, the energy of the lattice wells are alternately shifted up and down in energy by an amount of $\pm\delta$. Thus also the energies of the WS resonance states shift by an amount of $\pm\delta$ and the positions of the RET peaks changes by $\Delta F_{res} = \pm 2\delta/(2\pi)$, 2π being the period of the optical lattice.

The change of the peak height Γ_{res} in a bichromatic optical lattice is much more striking as shown in Fig. 7(c). The height of one of the RET peaks increases drastically for larger values of δ . For $\delta > 0.08$ one can no longer identify a single RET peak. As argued above RET occurs when the real parts μ of the eigenenergies of two WS resonances cross, while the imaginary parts Γ anticross. For $\delta > 0.08$ the crossing scenario changes; the imaginary parts show a real crossing while the real parts anticross. The two different scenarios are commonly referred to a type I (real-parts cross) and type II crossing (imaginary parts cross), respectively [12,41,42]. The qualitative difference is also observed in the decay curves plotted in Fig. 7(a).

For both types of crossings, the eigenenergies are never fully degenerate—such a full degeneracy occurs only for isolated points in parameter space. At these exceptional points, already small nonlinearities lead to significant changes of the WS resonance states and especially their decay rates Γ . Examples are shown in Fig. 8 for $\delta = 1$ and different relative phases ϕ of the two lattices. An ordinary type II crossing is observed for $\phi = -1.7$, leading to the familiar RET peaks of the decay rates. Changing the phase slightly to $\phi = -1.6$ changes the type of the crossing scenario to type I. An exceptional point

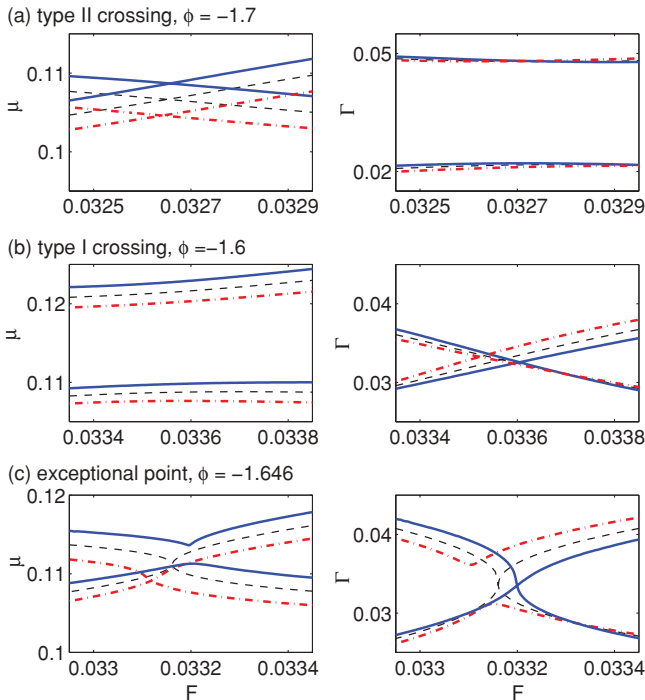


FIG. 8. (Color online) Chemical potential μ and decay rates Γ for (non-)linear WS resonances in a bichromatic optical lattice for $V_0 = 1/2$, $\delta = 1$ and (a) $\phi = -1.7$, (b) $\phi = -1.6$, (c) $\phi = -1.646$ and $g = 0$ (dashed black line), $g = +0.01$ (thick blue line), and $g = -0.01$ (dash-dotted red line).

is found for $\phi = -1.646$, as shown in Fig. 8(c). However, the degeneracy is lifted as soon as the atoms start to interact. A weak repulsive nonlinearity $g = +0.01$, turns the exceptional crossing into an ordinary type I crossing, while an attractive

nonlinearity $g = -0.01$ favors a type II crossing. This change of peak shape can have dramatic effects on the dynamics of a Bose-Einstein condensate, in particular when experimental parameters are adiabatically varied (see, e.g., Ref. [42]).

V. CONCLUSIONS

Bose-Einstein condensates in tilted optical lattices are ideal to study the decay of interacting open quantum systems. Experimentally the parameters can be tuned over a wide range and the dynamics can be recorded in situ. Here we presented an *efficient* method to calculate the decay rate in the mean-field regime also in the presence of degeneracies which also, unlike previous methods, is not restricted to ground-state calculations. The effects of the nonlinearity are strongest in the regime of resonant tunneling, where the decay rate can be enhanced by orders of magnitude by resonant coupling to unstable excited states. The interactions shift and bend the resonance peaks and eventually lead to a bistable peak shape. Even more interesting effects can be studied in tilted bichromatic lattices, where different types of level crossing scenarios emerge when the lattice parameters are tuned. These effects will be studied in detail in a future publication.

ACKNOWLEDGMENTS

We acknowledge financial support by the Deutsche Forschungsgemeinschaft (DFG) via the Graduiertenkolleg 792, the Forschergruppe 760 (Grant No. WI 3426/3-1), the Heidelberg graduate school of fundamental physics (Grant No. GSC 129/1) and the research fellowship program (Grant No. WI 3415/1-1). K.R. acknowledges support from a scholarship of the Université Libre de Bruxelles.

-
- [1] F. Bloch, *Z. Phys.* **52**, 555 (1929).
 [2] C. Zener, *Proc. R. Soc. London* **137**, 696 (1932).
 [3] J. Zak, *Phys. Rev. Lett.* **20**, 1477 (1968).
 [4] G. H. Wannier, *Phys. Rev.* **181**, 1364 (1969).
 [5] J. Zak, *Phys. Rev.* **181**, 1366 (1969).
 [6] J. E. Avron, J. Zak, A. Grossmann, and L. Gunther, *J. Math. Phys.* **18**, 918 (1977).
 [7] B. P. Anderson and M. A. Kasevich, *Science* **282**, 1686 (1998).
 [8] M. Gustavsson, E. Haller, M. J. Mark, J. G. Danzl, G. Rojas-Kopeinig, and H.-C. Nägerl, *Phys. Rev. Lett.* **100**, 080404 (2008).
 [9] M. Ben Dahan, E. Peik, J. Reichel, Y. Castin, and C. Salomon, *Phys. Rev. Lett.* **76**, 4508 (1996).
 [10] M. Jona-Lasinio, O. Morsch, M. Cristiani, N. Malossi, J. H. Müller, E. Courtade, M. Anderlini, and E. Arimondo, *Phys. Rev. Lett.* **91**, 230406 (2003).
 [11] C. Sias, A. Zenesini, H. Lignier, S. Wimberger, D. Ciampini, O. Morsch, and E. Arimondo, *Phys. Rev. Lett.* **98**, 120403 (2007).
 [12] A. Zenesini, C. Sias, H. Lignier, Y. Singh, D. Ciampini, O. Morsch, R. Mannella, E. Arimondo, A. Tomadin, and S. Wimberger, *New J. Phys.* **10**, 053038 (2008).
 [13] A. Zenesini, H. Lignier, G. Tayebirad, J. Radogostowicz, D. Ciampini, R. Mannella, S. Wimberger, O. Morsch, and E. Arimondo, *Phys. Rev. Lett.* **103**, 090403 (2009).
 [14] G. Tayebirad, A. Zenesini, D. Ciampini, R. Mannella, O. Morsch, E. Arimondo, N. Lörch, and S. Wimberger, *Phys. Rev. A* **82**, 013633 (2010).
 [15] M. Holthaus, *J. Opt. B: Quantum Semiclass. Opt.* **2**, 589 (2000).
 [16] M. Glück, A. R. Kolovsky, and H. J. Korsch, *J. Opt. B: Quantum Semiclass. Opt.* **2**, 694 (2000).
 [17] M. Glück, A. R. Kolovsky, and H. J. Korsch, *Phys. Rep.* **366**, 103 (2002).
 [18] S. Wimberger, R. Mannella, O. Morsch, E. Arimondo, A. R. Kolovsky, and A. Buchleitner, *Phys. Rev. A* **72**, 063610 (2005).
 [19] C. J. Pethick and H. Smith, *Bose-Einstein Condensation in Dilute Gases* (Cambridge University Press, Cambridge, 2008).
 [20] D. Witthaut, M. Werder, S. Mossmann, and H. J. Korsch, *Phys. Rev. E* **71**, 036625 (2005).
 [21] J. Liu, L. Fu, B.-Y. Ou, S.-G. Chen, D.-I. Choi, B. Wu, and Q. Niu, *Phys. Rev. A* **66**, 023404 (2002).
 [22] D. Witthaut, E. M. Graefe, and H. J. Korsch, *Phys. Rev. A* **73**, 063609 (2006).
 [23] T. Paul, K. Richter, and P. Schlagheck, *Phys. Rev. Lett.* **94**, 020404 (2005).

- [24] K. Rapedius, D. Witthaut, and H. J. Korsch, *Phys. Rev. A* **73**, 033608 (2006).
- [25] K. Rapedius and H. J. Korsch, *Phys. Rev. A* **77**, 063610 (2008).
- [26] N. Moiseyev and L. S. Cederbaum, *Phys. Rev. A* **72**, 033605 (2005).
- [27] P. Schlagheck and T. Paul, *Phys. Rev. A* **73**, 023619 (2006).
- [28] S. Wimberger, P. Schlagheck, and R. Mannella, *J. Phys. B* **39**, 729 (2006).
- [29] P. Schlagheck and S. Wimberger, *Appl. Phys. B* **86**, 385 (2007).
- [30] D. Witthaut, E. M. Graefe, S. Wimberger, and H. J. Korsch, *Phys. Rev. A* **75**, 013617 (2007).
- [31] K. Rapedius and H. J. Korsch, *J. Phys. B* **42**, 044005 (2009)
- [32] N. Moiseyev, L. D. Carr, B. A. Malomed, and Y. B. Band, *J. Phys. B* **37**, L193 (2004).
- [33] M. Glück, A. R. Kolovsky, and H. J. Korsch, *Eur. Phys. J. D* **4**, 239 (1998).
- [34] N. Moiseyev, *Phys. Rep.* **302**, 212 (1998).
- [35] A. U. J. Lode, A. I. Streltsov, O. E. Alon, H.-D. Meyer, and L. S. Cederbaum, *J. Phys. B* **42**, 044018 (2009).
- [36] A. Görlitz, T. Kinoshita, T. W. Hänsch, and A. Hemmerich, *Phys. Rev. A* **64**, 011401(R) (2001).
- [37] S. Fölling, S. Trotzky, P. Cheinet, M. Feld, R. Saers, A. Widera, T. Mueller, and I. Bloch, *Nature (London)* **448**, 1029 (2007).
- [38] G. Ritt, C. Geckeler, T. Salger, G. Cennini, and M. Weitz, *Phys. Rev. A* **74**, 063622 (2006).
- [39] T. Salger, C. Geckeler, S. Kling, and M. Weitz, *Phys. Rev. Lett.* **99**, 190405 (2007); *Science* **326**, 1241 (2009).
- [40] B. M. Breid, D. Witthaut, and H. J. Korsch, *New J. Phys.* **8**, 110 (2006); **9**, 62 (2007).
- [41] J. E. Avron, *Ann. Phys. (NY)* **143**, 33 (1982).
- [42] F. Keck, H. J. Korsch, and S. Mossmann, *J. Phys. A* **36**, 2125 (2003).